Metric for Comparing Lifetime Average Climate Impact of Aircraft

Emily Schwartz Dallara[*] and Ilan M. Kroo[†]
Stanford University, Stanford, California 94305
and
Ian A. Waitz[†]
Massachusetts Institute of Technology, Cambridge, Massachusetts 02139

The environmental impacts of commercial aviation, including climate change, are of growing importance in aircraft design. A framework is needed for comparing the climate impacts of competing aircraft designs and technologies. A metric is presented for this purpose: average temperature response. This metric quantifies the lifetime global mean temperature change caused by operation of a particular aircraft. This metric can be computed using any climate model. An example study of five aircraft using a linear climate model with altitude variation illustrates the range of climate performance for aircraft designed to the same requirements. For the particular example assumptions used, aircraft are designed with 10–50% lower average temperature responses and 1% higher operating costs relative to a minimum cost design. An uncertainty quantification study is also presented, demonstrating that uncertainty is not too great to make conclusions about the relative performance of different aircraft configurations.

Nomenclature

A_i	=	radiative efficiency of species i, $(W/m^2)/kg$
E_i	=	annual emissions rate of species i, kg/year
EI_i	=	emissions index of species i, kg/kg
e_i	=	emissions of species i per mission, kg
f_i	=	efficacy of species i
H	=	operating lifetime, years
h	=	altitude, ft
L	=	mission distance, n mile
$l(h)$	=	fraction of fleet distance flown at altitude h
RF	=	radiative forcing, W/m^2
r	=	function devaluation rate
RF^*	=	normalized radiative forcing
S	=	climate sensitivity, K
s_i	=	forcing factor for species i
t	=	time, years
t_{max}	=	weighting function maximum integration period, years
U	=	aircraft utilization rate, number of missions per year, yr^{-1}
$w(t)$	=	weighting function
W_{fuel}	=	fuel consumption per mission, kg
ΔT	=	global mean temperature change, K
τ	=	time constant, years

Introduction

CONCERN about the environmental impacts of commercial aviation has grown over the past few decades as the industry continues to expand. Recent attention has focused on limiting aviation effects on the global climate. In 2005, aircraft operations were estimated to have produced 4.9% of the worldwide anthropogenic forcing that causes climate change [1]. This fraction is projected to grow over the next several decades [1].

Commercial aircraft cause climate change through physical mechanisms that are described in detail in [1–4]. These effects include emissions of the direct greenhouse gas carbon dioxide (CO_2) and other species that affect the radiative balance of the Earth system. Nitrogen oxides (NO_x) impact the climate in two important ways. First, NO_x produces ozone through a process with a short lifetime (O_{3S}), which is a warming effect. Second, over long timescales, NO_x enhances the destruction of the greenhouse gases methane (CH_4) and ozone (O_{3L}), which are cooling effects. At smaller magnitudes, emissions of water vapor (H_2O) and aerosols of soot and sulfate (SO_4) also directly influence climate. Finally, the effects of linear contrails and altered cirrus cloudiness, collectively referred to as aviation-induced cloudiness (AIC), are estimated to have a significant warming effect. Total radiative forcing (RF) from aircraft is a factor of two to four times greater than forcing due to CO_2 alone [3]. However, it should be noted that RF is an instantaneous measure that does not capture the integrated effects of a new unit of aviation emissions. For the time-integrated future impacts, the ratio of non-CO_2 to CO_2 effects is, in general, different: an issue we address further in this paper.

The climate effect of each species depends on ambient conditions and emission rate, radiative properties, and impact lifetime (which describes the timescales of an atmospheric perturbation). CO_2, NO_x, H_2O and particle emissions quantities, radiative efficiencies, and lifetimes vary by several orders of magnitude. So, to aggregate the total effects of all aircraft emissions, a climate model is needed. Global climate models (GCMs) compute the physical, chemical, and biological processes of each climate component on a time-varying three-dimensional global grid. The Intergovernmental Panel on Climate Change (IPCC) is confident in the ability of these models to accurately characterize climate responses on global and hemispheric scales [5]. However, their high computational costs makes GCMs poorly suited for aircraft conceptual design and uncertainty studies. Instead, the climate response from aircraft emissions can be estimated using a simple climate model, applying linear relationships derived from the results of more complex GCMs.

Given the significance of aviation climate change, it is important for the aircraft design community to have a meaningful method for comparing the climate impacts of various aircraft configurations and technologies. This estimation must account for the multiple radiatively active species that aircraft emit. This paper discusses metrics that can be applied to quantify the climate impacts of different aircraft designs, and it presents a methodology for estimating aircraft climate performance with a single candidate metric. Performance measurements with this metric and alternative impact-based metrics are shown to yield similar results. The candidate metric provides a framework for assessing relative performance and is

*Doctoral candidate (Corresponding author).
†Professor. Fellow AIAA.

paired with a climate model that can be continually refined to reflect advancements in knowledge of aircraft climate impacts.

Measuring Aviation Climate Change

Climate change is defined by the IPCC as "a change in the state of the climate that can be identified by changes in the mean and/or the variability of its properties, and that persists for an extended period, typically decades or longer" [6]. Climate properties for which the variation can indicate climate change include temperature, precipitation, humidity, soil moisture, sea surface temperature, and sea ice location and thickness. Global mean surface temperature change is predicted more easily than variation in other climate properties [7]. In this paper, discussion of climate change will refer to changes in globally averaged surface temperature, noting that the operation of commercial aircraft may also affect other climate properties.

In the case of commercial aircraft, emissions of CO_2, NO_x, H_2O, SO_4, and soot from fuel combustion alter both atmospheric composition and cloud properties. The causal sequence of emissions to the impacts and damages caused by climate change is shown in Fig. 1 (adapted from [8]). Atmospheric processes convert direct aircraft emissions into chemicals and clouds that change the balance of incoming and outgoing energies in the Earth-atmosphere system, producing RF. RF components then cause climate change, manifested as changes to global mean temperature, precipitation, sea level, etc. Next, climate change influences agriculture, coastal geography, and other systems. The likelihood of significant impacts on these systems as a function of temperature rise is discussed in [6]. Finally, climate change impacts can be quantified monetarily as damages or costs to society.

Along each step of the path shown in Fig. 1, variables can be identified that could serve as climate change metrics. Metrics based on lower steps in the figure are increasingly relevant in quantifying the potential effects of climate change sought to be avoided. However, these quantities are also increasingly uncertain and difficult to predict. When selecting a metric for measuring climate change, one must balance the relevance of the metric against the uncertainty its use leads to in making decisions.

Researchers have adopted numerous climate metrics to quantify the impacts of aviation emissions. The strengths and weaknesses of these metrics are reviewed in [7,9–15]. Many of these metrics have been applied widely to the comparison of impacts from different sectors, the prediction of impacts based on future emission scenarios, and the assessment of various technology and policy mitigation strategies. In this paper, we seek to identify a metric for comparing the climate impacts of various aircraft configurations. To narrow the set of possible aircraft design climate metrics, discussion will focus on the appropriate properties of a metric for this purpose.

Metric Properties

Measured Quantity

A climate metric could measure many different physical or economic values, ranging from mass of emissions, to RF, to temperature change, to impacts and damages, as shown in Fig. 1. For estimating the impacts of aircraft operations, the mass of radiatively active emissions is not a meaningful metric because of the wide variety of aircraft emissions that affect climate. For example, the timescales and intensity of climate impacts due to emissions of 1 kg of CO_2 are very different from those of 1 kg of NO_x; furthermore, AIC impacts are not simply related to a single emissions quantity. Because of this, emissions-quantity metrics are less useful for aircraft design studies.

Economic metrics evaluate the damages and abatement costs of different emissions scenarios. Several climate change studies have used economic metrics: for example, [16–19]. These economic metrics use damage functions that estimate the effects of climate change in terms of the consumption-equivalent value of both market and nonmarket goods [20]. Such models are highly uncertain: Nordhaus describes the damage function in his model as "extremely conjectural given the thin base of empirical studies on which it rests" [21]. Uncertainty in estimating damages is more challenging to quantify and greater in magnitude than that of physical metrics such as RF and temperature change. Furthermore, temperature change is a tangible measure of climate change that is more accessible than damage metrics, and many policies focus on the objective of temperature rather than social damages. For comparative studies, under certain restrictive assumptions described in [12], conclusions drawn using global cost potential and global temperature potential (GTP) metrics coincide. Additionally, because the purpose of this metric is for use in aircraft design, and not policy decisions, economic metrics are not necessarily preferred. To inform future policy decisions, it is important to measure each environmental impact (noise, local emissions, and climate change) and understand how environmental and economic performance can be changed in design. This paper focuses on climate impacts, and a physical metric is suitable to characterize climate performance. For these reasons, economic-based metrics will not be used herein for comparative aircraft design study.

Other climate properties include RF and temperature change. RF measures the net imbalance of incoming and outgoing energies in the Earth-atmosphere system caused by a perturbation. RF does not directly measure a change in climate behavior, but it instead quantifies the change in energy that produces changes in climate properties, including temperature and precipitation. Under certain restrictive assumptions, RF is directly related to changes in equilibrium surface temperature [3]. The primary limitation of RF is that it is an instantaneous metric that captures impacts from emissions at a single point in time; however, time-integrated RF metrics can be used to quantify lifetime impacts. Temperature change, on the other hand, is a direct measure of a change in global climate behavior. RF is therefore a less direct measure of the level of impact of aircraft emissions. RF has the advantage of lower scientific uncertainty compared with temperature change and has been widely applied in climate change research, including aviation studies by the IPCC. Both RF and temperature change are identified as potential candidates for the basis of an aircraft design climate metric.

Emissions Case

Most climate metrics are computed based on a specified, general emissions case. For instance, consider global warming potential (GWP) metrics. Sustained 100-year GWPs are calculated assuming
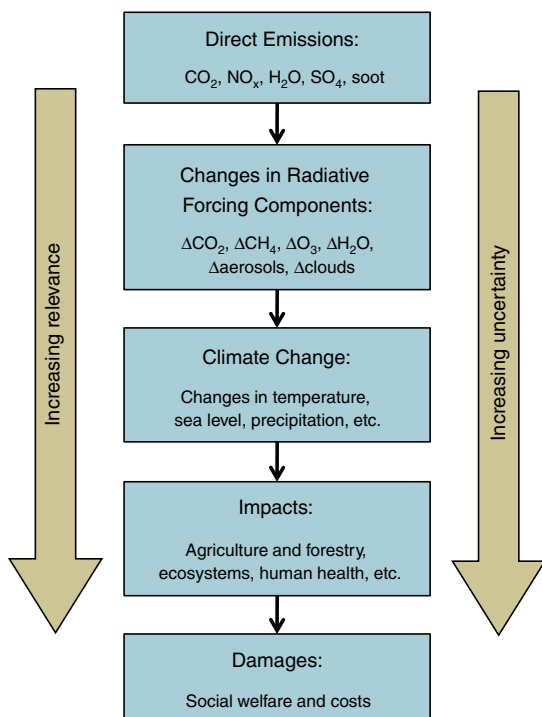

Fig. 1 Cause and effect chain for aircraft climate change, adapted from [8].

constant emissions for 100 years, while pulse 100-year GWPs are calculated assuming emissions for only one year and zero emissions thereafter. GWPs are used broadly for many applications and are also frequently referenced for 20-year and 500-year horizons. For the application of aircraft design, a more specific emissions case is appropriate. To compare the impacts of different aircraft designs, climate impacts can be computed with an emissions case representative of the likely operation of these designs. Based on typical commercial aircraft operation today, an appropriate emissions case might be constant operation for 30 years followed by aircraft retirement and zero emissions (other operating lifetimes could be considered for different aircraft design applications). The scenario of constant emissions during the operational lifetime and zero emissions thereafter is a simplistic representation of the emissions from a new aircraft design: in reality, new aircraft are adopted gradually and the net emissions rates from the new design change annually. However, this simple emissions case is sufficient to capture the differences in lifetime climate impacts in a comparative design study.

Snapshot Versus Integrated Impact

A climate metric can be based on the evaluation of a property at a single point in time or the integration of that property over a period of time. Common snapshot metrics include single-year RF and GTP, and common integrated metrics include GWP and integrated temperature change [14,15,19]. For aircraft design, a snapshot metric can be applied at the end of the operating lifetime, quantifying the value of a climate property near its peak value. Snapshot metrics could also be applied within the operating lifetime if considering a climate goal: for instance, a temperature change target in the year 2050. It should be noted that, even for a comparative study, snapshot metrics are very sensitive to timing, and a study with a lifetime of 10 years could give a different result than that with a lifetime of 50 years. Time-integrated climate metrics are less sensitive to lifetime and quantify mean impacts over an integration period. Because components of RF and temperature change are accumulative and vary annually, lifetime-averaged metrics are preferred.

Temporal Weighting

Given an integrated impact metric based on the emissions case described previously, the relative importance of short-lived and long-lived impacts can be altered by applying temporal weighting. Common methods for weighting include discounting and windowing, but other weighting functions can also be used. Discounting is frequently used in economic studies to express future value in present monetary terms and has been applied in climate change studies [19,22,23]. In a similar manner as discounting, weighting factors can be applied to a physical impact to specify the relative importance of immediate and far-future impacts. The integration window also affects this balance by setting the maximum time horizon for inclusion of impacts. Short-lived impacts decay quickly (10–30 years) after aircraft operations terminate, but long-lived impacts decay slowly (100s of years for CO_2). Therefore, an integration window that is long compared with the aircraft operating lifetime favors long-lived impacts, while a short window biases toward short-lived impacts. A weighting function can combine weighting factors and an integration window. Because choices of weighting represent judgments on the value of immediate and far-future impacts, an aircraft design climate metric should be flexible and allow user specification of the associated function.

Treatment of Uncertainty

Considerable uncertainty exists in the quantification of climate impacts from aircraft emissions and other sources. The relevant uncertainty may be categorized as described in [24]. Scientific uncertainty is associated with limits in scientific knowledge and inexact modeling approaches for estimating impacts from an emissions scenario. Valuation uncertainty exists because value judgments are required to temporally weight impacts. Scenario uncertainty refers to unknowns surrounding the projections of future anthropo-

genic activities and system responses that are required to estimate aircraft climate impacts. For an aircraft design climate metric to be practical, scientific uncertainty must be quantifiable. Scenario and valuation uncertainties should also be addressed by allowing user specification of trajectory and temporal weight assumptions.

Based on this discussion of the desired properties of an aircraft design climate metric, several metrics could be conceived. One such metric is presented in the following section.

Candidate Metric: Average Temperature Response

To compare the climate impacts of different aircraft designs, a metric is needed that appropriately characterizes the net global climate effect of the operation of a particular aircraft. We propose a metric and choose to base the metric on temperature change for several reasons. First, temperature change is commonly used within the climate modeling community but is also understood by non-experts. Second, it measures a physical change in climate behavior that could be controlled in order to limit climate change damages. The purpose of the candidate metric is to quantify for a particular aircraft the climate impacts realized from emissions during operation and climate impacts that result from perturbations remaining in the Earth-atmosphere system after the aircraft operating lifetime has ended.

The metric presented in this study is the average temperature response (ATR) over an aircraft operating lifetime. ATR combines integrated temperature change with the concept of temporal weighting and follows the general emissions metric formulation given in [5,18]. ATR is defined in Eq. (1):

$$\text{ATR}_H = \frac{1}{H} \int_0^\infty \Delta T_{\text{sust},H}(t) w(t) \, dt \qquad (1)$$

ATR is measured in units of temperature. The first step in computing ATR is calculating the global mean temperature change. In the preceding equation, $\Delta T_{\text{sust},H}$ refers to the time-varying global mean temperature change caused by H years of sustained operation of a particular aircraft configuration. The function $\Delta T_{\text{sust},H}(t)$ is determined based on constant annual emissions rates for the first H years of CO_2, NO_x, H_2O, soot, and sulfate, and then constant stage length and zero emissions thereafter. Aircraft operating lifetimes typically range between 25 and 35 years [3]. All studies herein assume an operating lifetime of 30 years.

Temperature change can be quickly calculated using a simple linear temperature response (LTR) model for aircraft conceptual design studies, or more sophisticated climate models can be used. LTR methods calculate the time-varying temperature change from a set of emissions using simplified expressions derived from the results of complex GCMs. LTRs of varying complexity have been applied to several aviation emissions studies [1,14,19,25–28].

Weighted temperature change per year is integrated and divided by H to yield an ATR. Any unitless weighting function may be used, and multiple functions could be appropriate for this purpose. Windowing and discounting are commonly applied [5,7,9–15,22]. Window weighting functions include only impacts occurring within a specified time frame, and an example of their application is the integrated RF metric GWP. Discounted metrics weight future impacts with an exponentially decaying function using either a constant or time-varying discount rate. Discount weighting functions are often applied in net present value economic metrics but can also be applied to physical metrics for many studies [29]. Conventional temporal weighting methods of windowing and discounting can be applied to an aircraft design climate metric, but other functions can also be used. To demonstrate this, the weighting function defined in Eq. (2) is presented:

$$w_r(t) = \begin{cases} 1 & t \leq H \\ \frac{1}{(1+r)^{t-H}} & H < t \leq t_{\max} \\ 0 & t_{\max} < t \end{cases} \qquad (2)$$

This function assigns unity weighting to temperature change during the operating lifetime of the aircraft. An exponential

devaluation rate is applied to temperature change occurring after the aircraft has ceased operation ($t \geq H$). A rate of zero means that postoperation impacts are equally important compared with impacts during operating years: a rate of infinity means that postoperation impacts have no importance; and a positive, finite rate means that temperature change each postoperation year is less important than the temperature change experienced the previous year. ATRs calculated using this weighting function are denoted as $\text{ATR}_{H,r}$ where H and r indicate the values of the operating lifetime and devaluation rate.

The function $w_r(t)$ is designed so that long-term effects are included but do not dominate ATR. As described by the IPCC, the design of a reduced climate impact next-generation commercial aircraft and other short-term climate abatement decisions involves "balancing the economic risks of rapid abatement now and the reshaping of the capital stock that could later be proven unnecessary, against the corresponding risks of delay" [30]. Designing an aircraft based on its climate impacts in 100 years is a higher risk than designing an aircraft based on its impacts in the next 30 years, because there is greater confidence that avoided climate change in the near term will be highly valued. The relative importance of a unit of temperature change in the far future is uncertain and unpredictable, and it depends on future trajectories of technological growth, realized physical impacts, and mitigation and adaptation. In contrast, the value of short-term impacts are more certain. We define short-term impacts by the window of approximately 30 years, which coincides with the operating lifetime of typical commercial aircraft. In Eq. (2), short-term impacts are weighted at unity, and long-term effects are weighted with importance, which decays exponentially. Decaying weighting factors are delayed 30 years for two reasons. First, as previously mentioned, scenario uncertainty is more moderate during this period: emissions, technological change, and policy scenarios are more certain for the next generation. Second, scientific uncertainty is lower during this period: results in [5] indicate that during a 30-year window, predictions of temperature change reasonably agree, not only within and across models but also between emissions scenarios.

This weighting function and other monotonically decreasing functions are consistent with approaching climate change abatement as a task of sequential decision-making under uncertainty [30]. The task is to design the next generation of commercial aircraft with cost-effective climate impact reduction solutions, so that in 30 years, climate change has not reached such high levels as to limit future options [31]. In the meantime, technology advancement and learning will continue. For the design of the following generation of aircraft, decisions will be better informed and aircraft climate mitigation will be reevaluated.

Selection of the weighting function involves a value judgment of the relative importance of short-lived and long-lived impacts. For the given weighting function, the devaluation is provided as a user-specified value judgment. Temperature change caused by short-lived impacts decays quickly after operation stops, while long-lived species such as CO_2 cause a residual temperature change for many years postoperation. In this paper, zero, moderate ($0 < r < 5\%$), and infinite rates will be considered. Discount rates of 2–5% are often applied in climate impact economic analyses [20]. The effect of changes to the devaluation rate on aircraft design decisions is explored in [32,33], where design conclusions are shown to be insensitive to choice of r (with a finite integration period). This insensitivity results because reductions in NO_x and AIC impacts are more easily achieved than reductions in CO_2 emissions. The integration window is taken to be very large compared with operating lifetime (if desired, shorter windows could also be used). A finite window is required for very low rates, because a fraction of CO_2 emissions remain in the atmosphere for many 1000s of years; therefore, most models for CO_2-induced temperature change do not decay to zero [34], and with larger rates, an infinite window is possible. For all examples in this paper, $t_{\max}$ is taken to be 500 years, following the longest time horizon adopted by the IPCC for GWP calculations [5]. Other devaluation rates, integration windows, and operating lifetimes can be applied; however, the same rates, windows, and lifetimes should be used when comparing two different design options.

The relationship between ATR with the presented weighting function and temperature change is shown graphically in Fig. 2 based on the commercial aircraft fleet emission rates in 2005, with $H = 30$ years and $r = 3\%$ [1]. Calculation of ATR for this emissions scenario represents the climate impacts that would result if every aircraft in the commercial fleet in 2005 was operated continuously until 2035 without fleet replacements or additions. This notional scenario illustrates the magnitudes and timescales of impacts of various aircraft emission components at current emissions rates. However, the ATR metric is designed for calculation of impacts for individual future aircraft configurations where the assumption of continuous emissions for 30 years is more realistic.

First, global mean temperature change is calculated assuming constant emission rates for the first H years and zero emissions thereafter, shown in Fig. 2a. Temperature change is computed using the linear climate model described in a later section of this paper. Next, the weighting function is applied to temperature change, reducing impacts occurring after H years, shown in Fig. 2b. Then, the weighted temperature change is integrated to find the total lifetime impact in units of Kelvins per year, represented by the shaded area in Fig. 2c. Finally, this quantity is divided by the operating lifetime to find the ATR, represented by the bar height in Fig. 2d. The shaded regions in Figs. 2c and 2d have equal area, $H \cdot \text{ATR}$. The notional 2005 fleet $\text{ATR}_{30,r=3\%}$ is approximately 35 mK.

To summarize, the ATR metric is proposed as a tool to condense the lifetime impacts of a particular aircraft into a single, meaningful quantity. The metric is designed for comparison of the lifetime temperature change of different aircraft design and technology options. This metric is not intended for use in aviation policy decisions or characterizing the absolute temperature change caused by operating a heterogeneous, evolving commercial aircraft fleet. By using a linear climate model, ATR can be calculated simply and quickly. Parameters and expressions in the linear climate model can be continuously updated to reflect best-available scientific knowledge of the effects of aircraft emissions. Additionally, by assessing the scientific uncertainty in the climate model, confidence in ATR calculations can be estimated. Uncertainty quantification will be discussed later in this paper.

Calculating Average Temperature Response

In this section, we describe a method for calculating the ATR of an aircraft. First, aircraft emissions are quantified. Then, using a climate model, emissions are translated into time-varying temperature change. Finally, ATR is computed and the uncertainty in this calculation is discussed. This study uses a LTR model with altitude-varying impacts, but other climate models could be used.

Aircraft Emissions

Total emissions of an aircraft over a specified mission are computed using the emissions index (EI), which is the mass ratio of emitted species to fuel burned, given in Eq. (3):

$$e_i = \text{EI}_i W_{\text{fuel}} \tag{3}$$

With this relationship, the mass of emitted species per mission can be found based on mission fuel consumption. The EIs of CO_2, H_2O, and $SO_4{}^{\ddagger}$ are solely dependent on the composition of the fuel and taken to be constants [3]. The EI for soot can vary with engine operating condition, but because soot comprises a small fraction of total climate impacts (on the order of less than 5%; see [4], for example), this factor can also be assumed constant without significant loss in accuracy for many studies of interest. These EIs are listed in Table 1.

The EI for NO_x depends strongly on operating conditions, including engine throttle setting. Engines are required to comply with NO_x emissions regulations during landing and takeoff. International Civil Aviation Organization (ICAO) measures and

---

‡This is an effective EI based on the EI of fuel sulfur [$\text{EI}(S) = 0.4$ g/kg] and a 50% effective conversion factor from fuel–sulfur to optically active sulfate aerosols [3].

a) Calculate $\Delta T_{\text{sust,H}}$

b) Apply weighting to $\Delta T_{\text{sust,H}}$ (affects only $t \geq H$ yrs)

c) Integrate weighted $\Delta T_{\text{sust,H}}$ (area = $H \cdot ATR$)

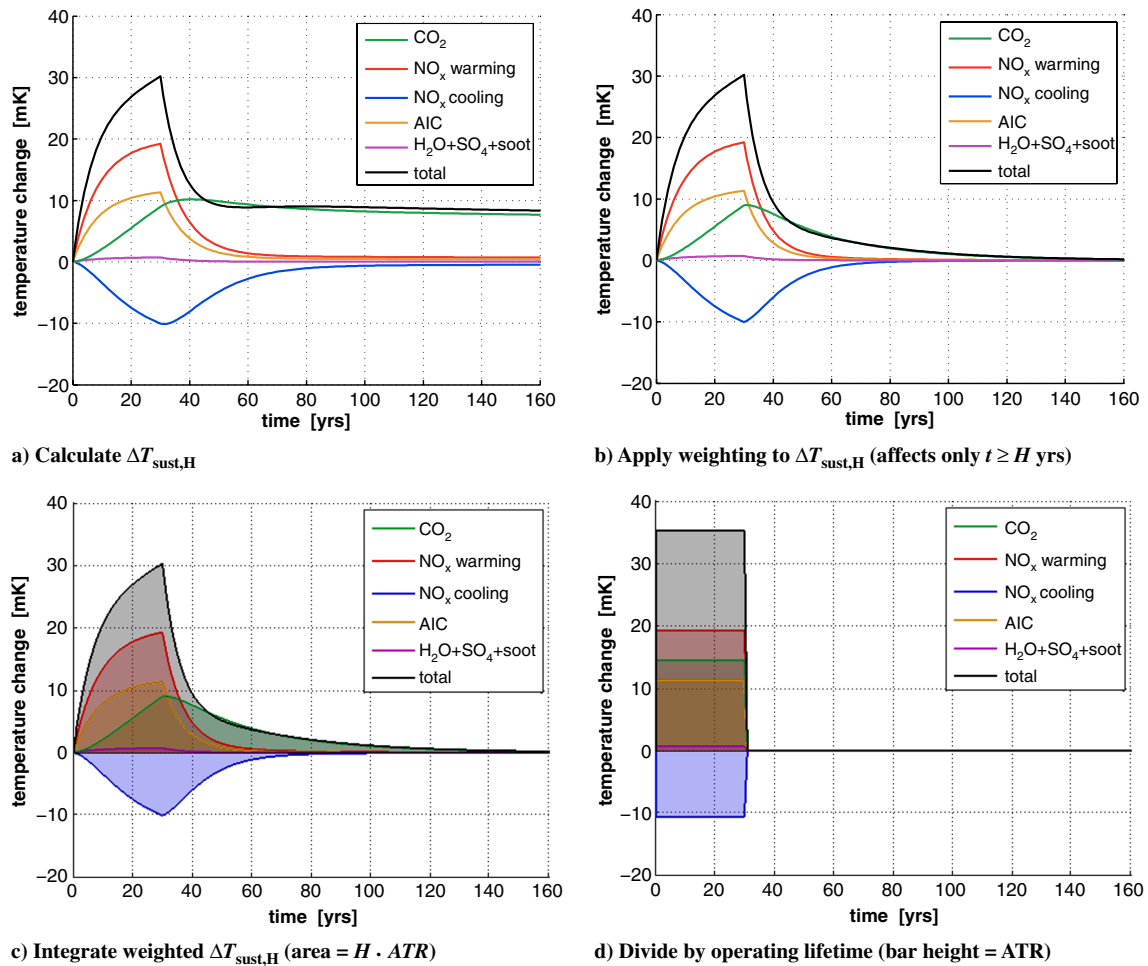**d) Divide by operating lifetime (bar height = ATR)**

Fig. 2   Graphical representation of steps for calculating ATR. In this example, $H = 30$ years, $r = 3\%$, and $t_{\text{max}} = 500$ years.

publishes certification data relating fuel flow, thrust, and EI_{NO_x} at four sea-level static throttle settings that simulate taxi, takeoff, climb, and approach operating conditions.[§] However, ICAO does not measure NO_x at cruise conditions, because these emissions are not currently regulated. Therefore, a model is needed to compute EI_{NO_x} at high altitudes based on sea-level static measurements. Fuel flow correlation methods have been developed for this purpose. The DLR, German Aerospace Center (DLR) method described in [35] is used in this study. This semiempirical method models the relationship between engine throttle setting and EI_{NO_x} at varying ambient temperature and pressure conditions. The DLR method has been shown to predict EI_{NO_x} to within approximately 10% of measurements at typical cruise conditions [36].

Once emissions over the design mission are estimated, the time-varying annual emissions rate is found by considering the aircraft utilization rate, shown in Eq. (4):

$$E_i(t) = e_i U(t) \qquad (4)$$

The utilization rate refers to the number of missions flown in year t.

Linear Climate Model with Altitude Variation

Once emissions rates are known, a climate model can be used to determine the temperature change resulting from aircraft operation. Any climate model can be used: options range from simple LTR models to complex three-dimensional GCMs. In this study, we employ the former option, which enables quick calculation of climate impacts and is appropriate for aircraft conceptual design.

Linear climate models have been developed to quantify emissions impacts and have been applied to several aviation emissions studies [1,14,19,25–28]. These models compute the impacts from emissions deposited by aircraft directly into the upper troposphere and lower stratosphere, which can lead to different climate impacts compared with ground-based emissions from other sectors. Although studies differ in how RF is computed for each pollutant, each of these studies relies on a similar methodology. First, emissions are computed and then translated into a time-varying RF of each species. Finally, a global mean temperature change is found by applying the forcing to a climate impulse response function. Because these models are derived from the results of one or more GCMs, linear models replicate the globally averaged results of the GCM(s) on which they are based. These climate models greatly simplify the physics and chemistry of aircraft-induced climate change, and the analysis generated by these models captures only first-order effects. The effects of varying background concentrations, latitude and longitude, timing, and interactions with other pollutants are not modeled. Scientific uncertainties associated with the modeling of climate responses are quantified within a Monte Carlo study. Impacts are computed based on current temporal and latitudinal flight distributions, and the effects of changes to routing, aside from altitude shifts, are beyond the scope of this paper.

Table 1   Emissions indices [3]

Species	Emissions index
CO_2	3.16 kg CO_2/kg fuel
H_2O	1.26 kg H_2O/kg fuel
SO_4	2.0e − 4 kg S/kg fuel
Soot	4.0e − 5 kg soot/kg fuel

The climate model developed for this study distinguishes itself from other linear climate models through its inclusion of altitude variation for NO_x, contrails, and cirrus impacts. This model relies on emissions impact studies published to date by the scientific community. However, model parameter best estimates are expected to change in the future and can be updated to reflect improved knowledge.

Radiative Forcing

Methods are provided for computing time-varying RF for each emitted species. Different models are required for long-lived gases, short-lived pollutants, and AIC. Models for RF from all emissions except CO_2, which has a very long atmospheric lifetime, are dependent on the assumed geographical distribution of emissions. The models described next are based on average impacts from fleetwide routing in a single year within the last decade. This routing is concentrated largely in the northern hemisphere midlatitudes. These models therefore quantify the average forcing caused by emissions spatially distributed according to routing similar to current traffic; if the geographical distribution of routes for a particular aircraft differs significantly from current routing, then these parameter values become less accurate.

The parameters used in this model are based on current best estimates, and many of these parameters are associated with large uncertainty. Uncertainty distributions for each of these parameters are listed in the Appendix.

Carbon Dioxide

Carbon dioxide is a well-mixed greenhouse gas with a long lifetime relative to chemical processes in the atmosphere. Because of this, aviation CO_2 impacts do not vary with altitude and can be treated in the same manner as all other anthropogenic CO_2 sources.

A relationship describing the RF caused by small perturbational emissions of CO_2 is given by the IPCC in [5], and it is shown in Eqs. (5) and (6). This linear model is based on the assumption of constant background CO_2 concentrations of 378 ppmv. This is an unlikely trajectory in the near term, and the impact of this scenario uncertainty is discussed later:

$$\mathrm{RF}_{CO_2}(t) = \int_0^t G_{CO_2}(t-\tau)E_{CO_2}(\tau)\,d\tau \tag{5}$$

$$G_{CO_2}(t) = A_{CO_2}\left\{1 + \sum_{j=1}^{3}\alpha_{cj}\left[\exp\left(\frac{-t}{\tau_{cj}}\right)-1\right]\right\} \tag{6}$$

In these equations, the expression $G_C(t)$ represents the decay of RF caused by a pulse emission of CO_2, measured in watts per meters squared per kilogram of CO_2. The portion of Eq. (6) in brackets describes the fraction of CO_2 emitted at $t = 0$, which remains in the atmosphere at time t [37]. Values of the parameters A_{CO_2}, α_{cj}, and τ_{cj} are listed in Table A1 of the Appendix.

Methane and Long-Lived Ozone

NO_x affects climate through ozone production/destruction and methane destruction. Ozone modeling must account for both short-term and long-term responses. In this section, the long-term forcings caused by methane destruction and ozone destruction are modeled.

Following [19], response functions G_i are derived for the RF from methane and long-term ozone destruction caused by a pulse emission of NO_x. These response functions are shown in Eq. (7):

$$G_i(t) = A_i\exp\left(\frac{-t}{\tau_n}\right) \quad \text{for } i = CH_4, O_{3L} \tag{7}$$

Values of the radiative efficiencies of methane and long-term ozone are calculated using the method described in [19], with results from [4,5,38]. Values of the radiative efficiencies A_{CH_4} and $A_{O_{3L}}$, and

the long-term ozone and methane adjustment time τ_n, are given in Table A2 in the Appendix.

The time-varying RF due to arbitrary emissions functions can then be computed using the response functions G_i. These response functions are derived based on fleetwide emissions and altitudes. By applying height-dependent forcing factors, RFs can be computed as altitude-specific values with Eq. (8):

$$\mathrm{RF}_i(t, h) = s_i(h)\int_0^t G_i(t-\tau)E_{NO_x}(\tau)\,d\tau \quad \text{for } i = CH_4, O_{3L} \tag{8}$$

Altitude-dependent forcing factors are unitless parameters that represent the RF per emission at a particular altitude, normalized by fleetwide average RF. These functions $s_i(h)$ are based on data for RF per emission as a function of altitude, as derived in [39], from perturbational studies of aircraft NO_x emissions. Separate NO_x forcing factors are applied to short-lived ozone RFs (described in the next section) and long-lived ozone and methane forcings. These data are normalized by the distance-weighted average RF per emission to define $s_i(h)$, shown in Eq. (9):

$$s_i(h) = \frac{(\mathrm{RF}_i/E_{NO_x})(h)}{\int_0^\infty(\mathrm{RF}_i/E_{NO_x})(h)l(h)\,dh} \quad \text{for } i = CH_4, O_{3L}, O_{3S} \tag{9}$$

The function $l(h)$ is the ratio of the distance flown by the commercial fleet at altitude h to the total distance flown and is based on the inventory used in [39]. It should be noted that $(\mathrm{RF}_i/E_{NO_x})(h)$ is not available for $h < 16{,}500$ ft, and $l(h)$ is nonzero in this range. To compute the denominator of Eq. (9), $(\mathrm{RF}_i/E_{NO_x})(h < 16{,}500$ ft$)$ is assumed constant and equal to $(\mathrm{RF}_i/E_{NO_x})(h = 16{,}500$ ft$)$. This assumption has a small effect on the magnitude of forcing factors: a shift of 10% in $(\mathrm{RF}_{O_{3S}}/E_{NO_x})(h < 16{,}500$ ft$)$ causes a change in $s_{O_{3S}}$ of less than 1%. This is because forcing factors are comparatively low at these altitudes and a small fraction of distance is flown below 16,500 ft.

Forcing factors for methane and long-lived ozone are plotted versus altitude in Fig. 3.

Short-Lived Emissions

Several aviation emissions have lifetimes much shorter than one year. Short-lived species include water vapor, short-lived ozone, soot, and sulfate aerosols. These species cause RF for only a short time after emission.

RF is assumed to be directly proportional to the RF per emission for a reference year, from [3,4]. This model averages and greatly simplifies the effects of the complex processes associated with
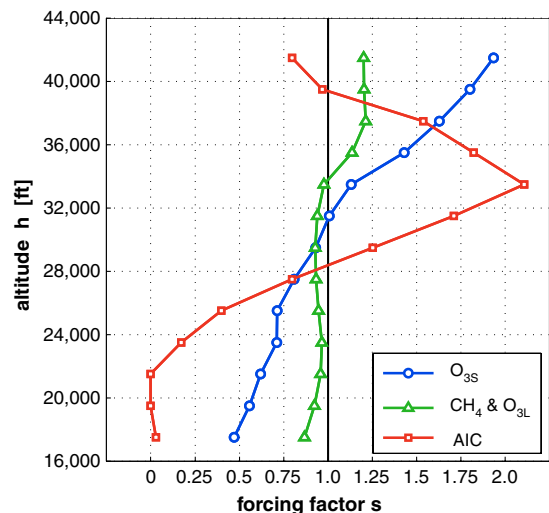

Fig. 3 RF factor data for NO_x impacts and AIC, based on results from [39,41].

forcing from NO_x-induced ozone production, leading to large uncertainty, which is addressed later:

$$RF_i(t, h) = s_i(h)\left(\frac{RF_{ref}}{E_{ref}}\right)_i E_i(t)$$

$$\text{for } i = H_2O, NO_x - O_{3S}, \text{soot, } SO_4 \tag{10}$$

Forcing factors are unity for all short-lived species except short-term ozone, for which the forcing factors are shown in Fig. 3 and computed using Eq. (9). Values of the parameters $(RF_{ref}/E_{ref})_i$ are listed in Tables A2 and A3 in the Appendix.

Aviation-Induced Cloudiness

AIC refers to the combination of contrails and aviation-induced cirrus clouds. AIC is also a short-lived effect. The linear model of RF due to contrails and cirrus relies on the basic assumption by Stordal et al. that a change in the cloud cover over an area is proportional to a change in aircraft flight distance [40]. Thus, AIC RF is assumed to be directly proportional to a reference AIC RF per distance traveled. This model does not reflect variation in AIC impact with changing water vapor emissions and exhaust temperature, and it will likely be refined in the future:

$$RF_{AIC}(t, h) = s_{AIC}(h)\left(\frac{RF_{ref}}{L_{ref}}\right)_{AIC} L(t) \tag{11}$$

In Eq. (11), L is the stage length flown per year. The value of the parameter $(RF_{ref}/L_{ref})_{AIC}$ is listed in Table A3 in the Appendix. AIC forcing factors are derived in a similar manner to the forcing factors of NO_x effects. AIC forcing factors are defined by Eq. (12) using data from [41]:

$$s_{AIC}(h) = \frac{(RF_{AIC}/L)(h)}{\int_0^\infty (RF_{AIC}/L)(h)l(h)\,dh} \tag{12}$$

The clouds forcing factor data from [41] were computed for contrails only. However, as noted in [42], cirrus cloud coverage is expected to scale with contrails to the first order. Therefore, the contrails forcing factor is applied to AIC RF.

Forcing factors for AIC and NO_x impacts are each based on data generated by a single GCM, and the effects of resulting uncertainties are quantified within a Monte Carlo study. These forcing factors characterize globally and annually averaged RFs based on current flight routes. Forcing factors, particularly for AIC impacts, are expected to vary diurnally, seasonally, and latitudinally, and quantification of these sensitivities is needed in future work.

Temperature Response

Before computing temperature change, RF for each species is converted into normalized RF. Normalized RF is adjusted based on each species efficacy parameter f_i and is divided by the RF that would result from a doubling of CO_2, shown in Eq. (13):

$$RF_i^*(t, h) = f_i \frac{RF_i(t, h)}{RF_{2xCO_2}}$$

$$\text{for } i = CO_2, CH_4, O_{3L}, O_{3S}, H_2O, \text{soot, } SO_4, \text{AIC} \tag{13}$$

Efficacy is a unitless parameter that compares the change in surface temperature for equal forcings of species i and CO_2 [5]. By definition, the efficacy of CO_2 is one. Efficacies are computed based on distributions of forcing from inventoried aircraft emissions and are assumed to be independent of altitude. Significant changes to flight routing could alter a species efficacy, but these sensitivities are expected to be small compared with the altitude dependencies of RFs. Values for efficacies and RF_{2xCO_2} are listed in Tables A2–A4 in the Appendix.

Once normalized RFs have been computed for each species, they are summed and applied to a climate impulse response function to find a time-varying global mean temperature change. Several climate impulse response functions have been developed for this

purpose [10,37,43,44]. In this study, we adopt the impulse response function of [37], which has two decay modes. These time constants describe the thermal response of the Earth system to an energy perturbation, measured by normalized RF, produced from any emissions species. Temperature change is calculated from RF* using Eqs. (14) and (15):

$$\Delta T(t) = \int_0^t G_T(t - \tau)\left[\sum_i RF_i^*(\tau)\right] d\tau$$

$$\text{for } i = CO_2, CH_4, O_{3L}, O_{3S}, H_2O, \text{soot, } SO_4, \text{AIC} \tag{14}$$

$$G_T(t) = S\left[\frac{\alpha_t}{\tau_{t1}}\exp\left(\frac{-t}{\tau_{t1}}\right) + \frac{1 - \alpha_t}{\tau_{t2}}\exp\left(\frac{-t}{\tau_{t2}}\right)\right] \tag{15}$$

In Eq. (15), the climate sensitivity parameter S is the steady-state temperature change that would result from a constant annual forcing of RF_{2xCO_2}. Values for each of the parameters S, τ_{t1}, τ_{t2}, and α_t are listed in Table A4 of the Appendix.

It should also be noted that this temperature change is based on a global mean response to RFs, which can be produced either globally or regionally. CO_2 has a long lifetime, allowing the gas to mix throughout the atmosphere so that RF is independent from emission location. Shorter-lived perturbations, such as ozone production from NO_x emissions, only cause RF near flight routes. Thus, RF due to O_3 production is greatest in the northern midlatitudes where aircraft traffic is most dense [3]. This study does not consider varying regional impacts from aircraft emissions and instead focuses on the climate response averaged over the Earth's surface. Regional impacts are uncertain and difficult to predict, even with GCMs [5]. Thus, at present regional climate impact, metrics are not appropriate for comparative aircraft design studies.

Average Temperature Response

With the linear climate model described previously, time-varying temperature change can be calculated for an arbitrary aircraft emissions scenario. To determine ATR, $\Delta T(t)$ must be calculated for the scenario of constant emissions during the first H years of operation and zero emissions thereafter. This yields the quantity $\Delta T_{sust,H}(t)$, defined in Eqs. (16) and (17):

$$\Delta T_{sust,H}(t) = \Delta T(t)|_{s_i = \bar{s}_i, E_i(t) = e_i U_{sust}\sigma_H(t)} \tag{16}$$

$$\sigma_H(t) = \begin{cases} 1 & t \leq H \\ 0 & H < t \leq t_{max} \end{cases} \tag{17}$$

In Eq. (16), the index i includes all radiatively active emissions and effects (CO_2, NO_x, H_2O, SO_4, soot, and AIC). Emissions rates are based on the performance of a particular aircraft on a specified mission. Utilization rate is assumed to be constant. The function $\sigma_H(t)$ in Eq. (17) is a unity backward step that characterizes the input emissions scenario. $\Delta T_{sust,H}(t)$ is calculated with mission-averaged forcing factors $\bar{s}_i$, computed with Eq. (18):

$$\bar{s}_i = \frac{L_{cruise}}{L_{total}}\left[\frac{1}{h_f - h_i}\int_{h_i}^{h_f} s_i(h)\,dh\right] + \left(1 - \frac{L_{cruise}}{L_{total}}\right)s_{i,low} \tag{18}$$

where $\bar{s}_i$ denotes the average forcing factor over the entire mission. This quantity is a weighted average of the forcing factors during the cruise and the climb/descent phases of the mission based on the fraction of mission stage length flown in each segment. The cruise forcing factor is calculated assuming a continuous cruise climb with initial and final cruise altitudes h_i and h_f, respectively. The forcing factors during climb and descent $s_{i,low}$ are based on NO_x forcing factors at $h_{low} = 16,500$ ft and an AIC forcing factor of zero. For current commercial aircraft on typical missions, a total distance of approximately 250 n mile is flown during climb and descent [45].

Once $\Delta T_{sust,H}$ is known, ATR with specified devaluation rate and operating lifetime can be computed with Eq. (1). However, because

Table 2   Values of unit ATRs for $H = 30$ years, $t_{max} = 500$ years, and four different values of r calculated with the linear climate model described in this paper

Species, i	$u\mathrm{ATR}_{30,r=0}(i)$	$u\mathrm{ATR}_{30,r=1\%}(i)$	$u\mathrm{ATR}_{30,r=3\%}(i)$	$u\mathrm{ATR}_{30,r=\infty}(i)$
CO_2, K per kg CO_2	1.66×10^{-13}	4.36×10^{-14}	1.96×10^{-14}	5.59×10^{-15}
CH_4, K per kg NO_x	-4.76×10^{-12}	-3.40×10^{-12}	-2.78×10^{-12}	-1.44×10^{-12}
O_{3S}, K per kg NO_x	9.46×10^{-12}	7.19×10^{-12}	6.46×10^{-12}	4.85×10^{-12}
O_{3L}, K per kg NO_x	-1.29×10^{-12}	-9.25×10^{-13}	-7.57×10^{-13}	-3.91×10^{-13}
H_2O, K per kg H_2O	5.77×10^{-15}	4.38×10^{-15}	3.94×10^{-15}	2.96×10^{-15}
SO_4, K per kg SO_4	-6.13×10^{-11}	-4.66×10^{-11}	-4.18×10^{-11}	-3.14×10^{-11}
Soot, K per kg soot	2.38×10^{-10}	1.81×10^{-10}	1.63×10^{-10}	1.22×10^{-10}
AIC, K per n mile	8.90×10^{-13}	6.76×10^{-13}	6.07×10^{-13}	4.56×10^{-13}

the climate model described herein is linear, $\mathrm{ATR}_{H,r}$ of multiple designs can be computed more simply by defining a new quantity: unit ATR of species i. The variable $u\mathrm{ATR}_{H,r}(i)$ is defined as the ATR resulting from H years of unit emissions (1 kg per year or 1 n mile per year) of only species i and excluding altitude effects, shown in Eq. (19). It should be noted that atmospheric processes are nonlinear, but globally averaged responses to small perturbations (in magnitude similar to commercial aircraft emissions) of CO_2, NO_x, and AIC perturbations have been shown to be nearly linear [1,39,41]. Response linearity is a fundamental assumption of the climate model described in the previous section, and the associated uncertainties in this formulation are captured in the scientific uncertainty quantification study:

$$u\mathrm{ATR}_{H,r}(i) = \mathrm{ATR}_{H,r}\big|_{s_i=1,E_j(t)=\sigma_H(t)} \quad \text{if } i=j \quad \text{and} \quad 0 \text{ otherwise}$$
(19)

With these unit ATRs precomputed, $\mathrm{ATR}_{H,r}$ becomes a simple summation for given utilization rate, cruise altitudes, and emissions per flight, as in Eq. (20). Emissions per flight for a current aircraft can be estimated based on mission fuel consumption and overall NO_x EI (which can be computed from published landing–takeoff emissions using an empirical method):

$$\mathrm{ATR}_{H,r} = U_{\mathrm{sust}} \sum_i \bar{s}_i e_i u\mathrm{ATR}_{H,r}(i)$$
(20)

Unit ATRs are calculated for several devaluation rates, an operating lifetime of 30 years, and a maximum integration period of 500 years in Table 2.

Uncertainty Quantification

As previously discussed, a number of sources of uncertainty exist in estimating the ATR of an aircraft. Scientific modeling uncertainty is quantified in the sections to follow. Other sources include valuation and scenario uncertainty. The selection of a temporal weighting function and its associated parameters affects the relative importance of short-term and long-term impacts, and therefore involves valuation uncertainty. This uncertainty is not assessed, and these judgments are instead presented as user-specified inputs in the ATR framework. Scenario assumptions are implicit in the linear climate model presented in this paper. The linear CO_2 RF model assumes constant background concentrations. The impact of this assumption is investigated by comparing results with a model with varying background concentrations. The climate model also assumes that physical climate responses will not change in the future: that climate feedback mechanisms and all species radiative efficiencies remain constant. This uncertainty is not quantified in this study and relates to future scenarios, which are difficult to predict. Scenario judgments are also provided as user-specified inputs through the selection of a climate model.

Next, the method for quantifying scientific uncertainty in ATR estimation is discussed. By analyzing the uncertainty in each component of the climate model, information can be determined about the uncertainty in outputs from the model. Exact values of parameters used in the linear climate model are not known; instead, parameters can be more appropriately described by probability distributions over the range of possible parameter values. Distribution information for model parameters used in this study are given in the Appendix in Tables A1–A4.

Following [1], the uncertainties in NO_x-induced RF parameters $[A_{CH_4}, A_{O_{3L}}, \text{and} (\mathrm{RF}_{\mathrm{ref}}/E_{\mathrm{ref}})_{O_{3S}}]$ are likely to be linked. Correlation coefficients of 0.5 are assumed between these three parameters. All other uncertain parameters are assumed to be independent.

Uncertainties in forcing factor functions are based on uncertainty in data for $(\mathrm{RF}_i/E_{NO_x})(h)$ and $(\mathrm{RF}_{\mathrm{AIC}}/L)(h)$ from [39,41]. This information is used to calculate $s_i(h)$ via Eqs. (9) and (12). The probability distributions for $(\mathrm{RF}_{CH_4}/E_{NO_x})(h)$ and $(\mathrm{RF}_{O_{3S}}/E_{NO_x})(h)$ are assumed to be normal, with a 66% likelihood each parameter is within $\pm15\%$ of the published value. These distributions are inferred from results in [46], where the change in NO_x impacts for altitude shifts of $+2,000$ and $-6,000$ ft were assessed by multiple climate models. The altitude-dependent component of $(\mathrm{RF}_{\mathrm{AIC}}/L)(h)$ is assumed to be normally distributed with a 90% likelihood that the value is within $\pm70\%$ of the published result.¶

While there is uncertainty in, for example, $(\mathrm{RF}_{O_{3S}}/E_{NO_x})(h)$ at each altitude h, it is likely that uncertainty at a particular altitude is closely related to uncertainty at nearby altitudes. That is to say, it is unlikely that the actual value of $(\mathrm{RF}_{O_{3S}}/E_{NO_x})(h)$ at 25,000 ft is 15% lower and at 27,000 ft is 15% higher than the data published in [41]. To account for this, this study assumes that uncertainties in $(\mathrm{RF}_i/E_{NO_x})(h)$ and $(\mathrm{RF}_{\mathrm{AIC}}/L)(h)$ are independent in 8000 ft intervals. Specifically, the uncertainties of these parameters at 17,500, 25,500, 33,500, and 41,500 ft are independent, and the uncertainty at altitudes between these levels is based on a linear variation between the nodes. To calculate forcing factors $s_i(h)$ based on uncertain values of $(\mathrm{RF}_i/E_{NO_x})(h)$ and $(\mathrm{RF}_{\mathrm{AIC}}/L)(h)$, this information is renormalized via Eqs. (9) and (12) so that the distance-weighted integral of s_i remains unity. Figure 4 shows the 66% likelihood ranges based on this method for $s_{O_{3S}}$, s_{CH_4}, and s_{AIC}.

Once probability distributions for model parameters are known, scientific uncertainty can be studied. In this paper, Monte Carlo analysis with Latin hypercube sampling is performed using the Design Analysis Kit for Optimization and Terascale Applications (DAKOTA) software package [47]. Paired Monte Carlo analysis, described in [24], is used to estimate only the uncertainty, which is relevant for comparative study. This analysis relies on a large number of trials of calculating ATR with random values from each parameter's probability distribution. A sufficient number of trials are computed so that the output distribution converges. Sensitivity analysis can also be performed using DAKOTA to quantitatively determine the effect of uncertainty in each model input parameter on the variance in ATR. This study uses variance-based decomposition methods described in [48].

Example

Next, an example is presented comparing the climate performance of several configurations. Five aircraft meeting the same takeoff, climb, cruise, and landing requirements are compared. Each of these aircraft carries 162 passengers over a maximum range of 3000 n mile

---

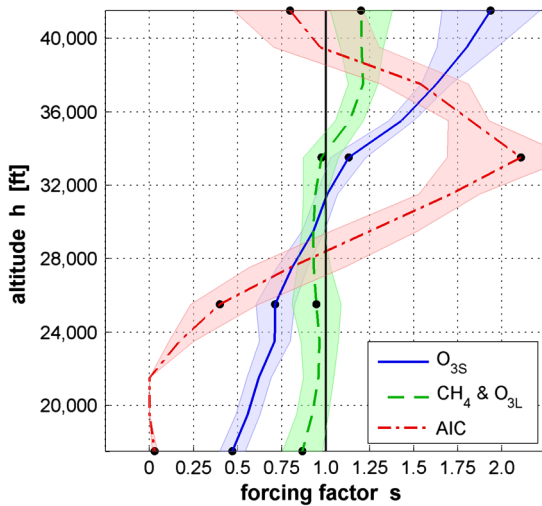¶G. Rädel, personal communication, 2009.

Fig. 4 Forcing factors (lines) with 66% likelihood ranges (shaded areas). Altitudes with forcing factors based on radiative forcing data with independent probability distributions are marked with black points.

and meets performance requirements similar to those of a 737-800. Designs A, B, C, and D were generated for the study presented in [49]. These aircraft were designed to illustrate the tradeoff between designing for low operating costs and low climate change impact. Design E is a new configuration.

Performance of these designs is estimated using the Program for Aircraft Synthesis Studies aircraft conceptual design tool [50]. This tool integrates a set of industry design methods to compute aircraft performance, including operating costs, fuel consumption, emissions, and ATR based on aircraft design variables. Technology levels for these aircraft, including engine NO_x emissions indices, are assumed to be consistent with an entry into service of 2010. Total

operating cost estimates are based on 2008 labor rates and a fuel price of $2.50 per gallon.
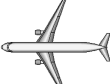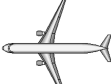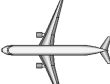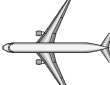
Characteristics of the five aircraft designs are shown in Table 3. Design A corresponds to an aircraft designed exclusively for minimum operating costs. Designs B, C, and D are designed for low operating costs and increasingly low climate change impacts. These aircraft tend to cruise more slowly and at lower altitudes than the current fleet to reduce impacts from ozone and AIC. Design E is designed to have low climate impacts excluding the effects of AIC. This aircraft will be discussed separately. Top-view images of these aircraft are shown, illustrating the similarity between these designs and conventional aircraft flying today.

Table 3 also shows the environmental and economic performances of the five designs. Performance results are based on a typical mission with a 100% load factor, no additional cargo, and a stage length of 1000 n mile. ATR, fuel burn, emissions, and operating costs are all shown relative to the reference minimum cost aircraft: design A. The utilization rate of each of these aircraft is equal. Because relative performance is assessed and a linear climate model is used, the value of utilization rate has no effect on performance results. $ATR_{H,r}$ values are determined using the climate model with the best estimate parameter values, which are listed in the Appendix. An uncertainty study taking into account model parameter distributions will be discussed later.

First, we examine the $ATR_{30,r}$ of design A for various devaluation rates. For $r = 0$, CO_2 impacts are very significant, comprising 62% of ATR. Long-term impacts (CO_2, CH_4, and O_{3L}) become less important for nonzero rates. At devaluation rates of 1 and 3%, CO_2 impacts account for 35 and 21% of ATR, respectively. Nearly all of the remaining ATR is caused in approximately equal portions by NO_x and AIC impacts. Small short-term impacts from H_2O, SO_4, and soot combine to contribute on the order of 1% of design A's ATR. Finally, for $r = \infty$, only 8% of the aircraft ATR is attributable to CO_2, and NO_x and AIC each contribute nearly 50%.

Comparing the relative $ATR_{30,r=0}$ of designs A–D, it is clear that flying at lower altitudes enables a significant reduction in AIC and net

Table 3 Description and performance of five aircraft on a typical 1000 n mile mission designed with a payload of 162 passengers and a maximum range of 3000 n mile

	Design A	Design B	Design C	Design D	Design E
Design description					
Maximum takeoff weight, lb	157,000	153,000	152,000	151,000	155,000
Wing area, ft^2	1320	1150	1120	1080	1220
Wing aspect ratio	9.1	11.2	11.9	13.3	10.2
Wing sweep, deg	36	28	26	21	32
Sea-level-static thrust, lb	22,900	21,700	21,300	20,600	22,200
Engine bypass ratio	9.0	9.5	9.7	10.7	9.4
Cruise Mach number	0.85	0.78	0.76	0.71	0.81
Initial/final cruise altitude, kft	37/39	28/31	26/28	22/23	33/35
Performance					
Relative $ATR_{30,r=0}$	1	0.89	0.79	0.69	1.03
Fraction of $ATR_{30,r=0}$ from $CO_2/NO_x/AIC$, %[a]	62/16/22	71/6/22	81/4/14	97/0/1	60/9/30
Relative $ATR_{30,r=1\%}$	1	0.80	0.62	0.43	1.05
Fraction of $ATR_{30,r=1\%}$ from $CO_2/NO_x/AIC$, %[a]	35/28/36	45/13/41	59/10/30	89/4/4	34/16/49
Relative $ATR_{30,r=3\%}$	1	0.76	0.54	0.30	1.05
Fraction of $ATR_{30,r=3\%}$ from $CO_2/NO_x/AIC$, %[a]	21/36/42	28/19/51	40/18/40	74/16/6	20/21/58
Relative $ATR_{30,r=\infty}$	1	0.73	0.50	0.26	1.04
Fraction of $ATR_{30,r=\infty}$ from $CO_2/NO_x/AIC$, %[a]	8/47/44	12/31/56	17/36/45	35/53/8	8/30/61
Relative fuel burn	1	1.02	1.04	1.08	1.00
Relative NO_x emissions	1	0.97	1.00	1.08	0.94
EI_{NO_x}, g/kg	21.7	20.6	20.8	21.6	20.5
Ozone forcing factor	1.37	0.82	0.72	0.61	1.03
Methane forcing factor	1.12	0.92	0.92	0.94	0.99
AIC forcing factor	1.04	0.97	0.54	0.05	1.51
Average cruise velocity, kt	487	458	450	434	467
Relative total operating costs	1	1.008	1.012	1.023	1.002

[a]Percentages do not add to 100 because of rounding and because small forcings (H_2O, soot, and sulfate) are not included.

NO_x impacts. Designs B, C, and D have 11, 21, 31% lower $ATR_{30,r=0}$ compared with design A, primarily due to the effect of reduced O_{3S} and AIC forcing factors. Design D cruises at 22,000 ft, where NO_x and AIC impacts are essentially eliminated. The cost of flying at lower altitudes is increased fuel burn (between 2 and 8% increase) and total operating costs (0.8 to 2.3%). However, the reduction in climate impacts from NO_x and AIC impacts easily exceeds the effects of increased CO_2, even with a devaluation rate of zero.

With devaluation rates of 1 and 3%, the effects of reduced altitude are more pronounced, since short-term impacts become dominant. Between a 20 and 70% reduction in ATR is attainable with designs B, C, and D at these rates. With an infinite devaluation rate, design D has nearly three-quarters lower ATR than the reference design.

The benefits of decreasing cruise altitude for NO_x-caused ATR diminishes somewhat with increased devaluation rate. For $r = 0$, ATR from NO_x is completely eliminated, while for $r = \infty$, this effect is only reduced by approximately two-thirds. This is because warming effects (O_{3S}) from NO_x are short term, and cooling effects (CH_4 and O_{3L}) are long term. High devaluation rates are biased toward short-term impacts, and therefore NO_x warming; and low rates are biased toward long-term impacts and NO_x cooling. This net NO_x effect is also sensitive to the choice of weighting function, and relative performance improvements will change for different function structures.

Design E is designed to have reduced climate impacts as measured under a different set of assumptions. This aircraft is optimized to have low cost and low impact from CO_2 and NO_x emissions but excluding the effects of AIC. This notional example represents the aircraft that might be designed if either scientists discovered forcing due to AIC is close to zero or a technology was developed to eliminate the impacts AIC without penalty to aircraft efficiency (for example, an operational contrail avoidance strategy that reduces impacts from AIC with small fuel burn penalties, described in [45,51]). Estimation of the performance effects of specific climate mitigation technologies, including operational contrail avoidance and adoption of alternative fuels, is beyond the scope of this paper and is explored in [32,33].

Design E cruises at a slightly lower altitude than design A to reduce NO_x impacts. At this altitude, AIC impacts would be very severe if included in ATR. Design E also flies slower, with a slightly higher wing aspect ratio and engine bypass ratio and a lower wing sweep, resulting in a very small reduction in fuel burn compared with design A. Because of longer flight times, design E has 0.2% higher total operating costs. If AIC impacts are included, the ATR of design E is between 3 and 5% higher than that of design A, depending on the devaluation rate. However, by excluding AIC impacts, design A's ATR is reduced by 22–44% and design E's is reduced by 30–61%. The net result is that the ATR_{no-AIC} of design E is between 8 and 28% lower than the ATR_{no-AIC} of design A. This configuration demonstrates that if AIC effects could be eliminated, additional reductions in ATR could be achieved with a very low increase in

operating costs via small reductions in cruise altitude and Mach of 4000 ft and 0.04.

We also consider the scenario of designing a configuration for minimum cost but operating the aircraft at a lower altitude to reduce climate impact. In this example, design A (designed to fly at 37,000–39,000 ft) is instead flown at the cruise altitudes of design B (28,000–31,000 ft), denoted as design A*. Two cruise Machs are considered: Mach 0.85 and Mach 0.78. Performance results on these two missions are summarized in Table 4. These data show that, by slowing down, design A* achieves nearly the same ATR reductions as design B. Without slowing down, up to half of the ATR reduction is lost. Furthermore, without slowing down, the aircraft's maximum range decreases from 3000 to 2838 n mile. Because this aircraft was not designed to fly at lower altitudes and speeds, design A* has operating costs that are 0.2% higher at Mach 0.85 or 0.9% higher at Mach 0.78 than design B. Thus, flying an aircraft designed for conventional cruise altitudes at both lower altitude and lower speed can enable significant reductions in climate impact, but this is not as cost- or fuel-efficient as designing an aircraft for flight at these reduced altitudes.

Next, the impact of scientific modeling uncertainty on ATR calculations is considered. An uncertainty study is performed using paired Monte Carlo analysis with Latin hypercube sampling. For each trial, ATR is calculated for designs A, B, C, and D using the same set of random model parameter values. All model parameters and forcing factor functions are assumed to be uncertain, except the climate sensitivity parameter S, applied in Eq. (15). This parameter is simply a scaling factor that is applied to all calculations of ATR, and its uncertainty is not relevant for comparing relative impacts of different designs.

From the Monte Carlo analysis, we examine the variation in the reduction in ATR, $ATR_{30,r}(A) - ATR_{30,r}(j)$. By quantifying the uncertainty in the ATR reduction of each design as opposed to the uncertainty in the absolute ATR of each design, only the uncertainty relevant to the differences between the designs is captured. Uncertainty in ATR reduction is more appropriate for comparative study. For example, if two aircraft have identical fuel burn and fly at identical altitudes, but they have different NO_x emissions indices, the uncertainty in ATR reduction between the two designs solely depends on uncertainty in components of the climate model related to NO_x impacts. If, on the other hand, the uncertainty in absolute ATR is examined, uncertainty in all components of the climate model (CO_2, AIC, etc.) is included; a large portion of this uncertainty affects both designs identically and is extraneous in a comparative study.

In Fig. 5, bars indicate the ATR of designs A, B, C, and D calculated with best estimate model parameters. Error bars show the 66% likelihood ranges and the median value for the reduction in ATR compared with ATR (design A). Results are normalized so that the ATR of design A is unity, and they are shown for devaluation rates of 0% (left) and 3% (right).

Table 4   Performance of design A operating at its design point of 37,000–39,000 ft and at lower altitudes of 28,000–31,000 ft (design A*) on a typical 1000 n mile mission

	Design A	Design A* (Mach 0.85)	Design A* (Mach 0.78)
Performance			
Relative $ATR_{30,r=0}$	1	0.95	0.91
Fraction of $ATR_{30,r=0}$ from $CO_2/NO_x/AIC$, %[a]	62/16/22	72/7/21	71/6/22
Relative $ATR_{30,r=3\%}$	1	0.80	0.76
Fraction of $ATR_{30,r=3\%}$ from $CO_2/NO_x/AIC$, %[a]	21/36/42	29/21/48	29/19/51
Relative fuel burn	1	1.09	1.04
Relative NO_x emissions	1	1.15	0.96
EI_{NO_x}, g/kg	21.7	23.0	20.1
Ozone forcing factor	1.37	0.82	0.82
Methane forcing factor	1.12	0.92	0.92
AIC forcing factor	1.04	0.97	0.97
Average cruise velocity, kt	487	501	458
Relative total operating costs	1	1.010	1.017

[a]Percentages do not add to 100 because of rounding and because small forcings (H_2O, soot, and sulfate) are not included.
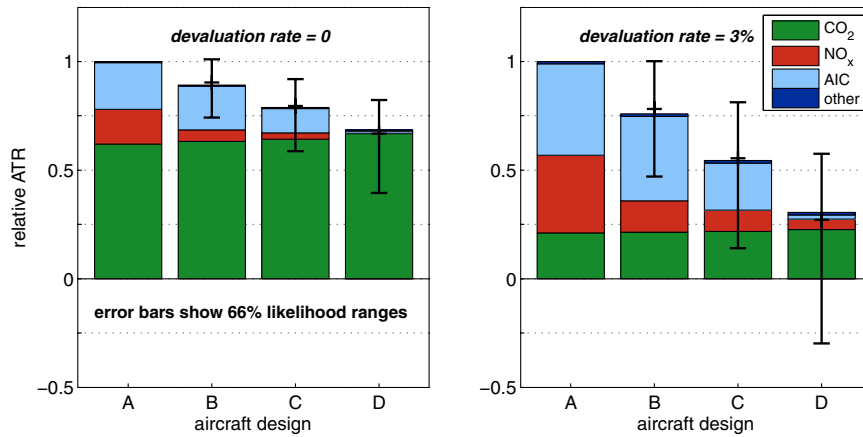
Fig. 5 Relative ATR of four aircraft designs for $r = 0$ (left) and $r = 3\%$ (right). Error bars indicate 66% likelihood range and median value of ATR reduction, $\mathrm{ATR}(A) - \mathrm{ATR}(j)$.

Figure 5 demonstrates that scientific uncertainty is not too large to make conclusions about the relative performance of competing designs. There is at least an 83% likelihood that designs B, C, and D have lower ATRs than design A. The figure also shows that the uncertainty ranges for $r = 3\%$ are larger than the ranges for $r = 0$. This occurs because the magnitudes of reductions in $\mathrm{ATR}_{r=3\%}$ are greater, and the likelihood ranges scale with reduction size. The $\mathrm{ATR}_{r=3\%}$ of design A is dominated by NO_x and AIC, and the considerably smaller $\mathrm{ATR}_{r=3\%}$ of designs B, C, and D illustrate the powerful effect of altitude reduction to reduce NO_x and AIC impacts, which is traded for a much smaller increase in CO_2 impacts.

The 66% likelihood ranges are not symmetric about the median value. Instead, very large ATR reductions are more probable than very small reductions. This is the case because the most significant differences between design A and designs B, C, and D lie in NO_x and AIC impacts; the RF parameters for both of these effects are lognormally distributed, which leads to higher probability of large savings for lower altitude flight.

Sensitivity analysis is performed using variance-based decomposition methods with the software package DAKOTA [47,48]. This analysis indicates that the uncertain model parameter that causes the largest variation in ATR reduction is $(\mathrm{RF}_{\mathrm{ref}}/E_{\mathrm{ref}})_{O_{3S}}$. For designs B and C, the parameter contributing the most to uncertainty in ATR reduction is s_{aic} at altitudes over 20,000 ft. For design D, this parameter is $(\mathrm{RF}_{\mathrm{ref}}/L_{\mathrm{ref}})_{\mathrm{AIC}}$. The importance of the uncertainty in these parameters is not surprising, since these parameters describe the primary differences between design A and designs B, C, and D. Improved knowledge about the values of these parameters will allow increased confidence in the comparison of ATRs of different aircraft.

Next, the effect of the background CO_2 scenario uncertainty is considered. Results from the CO_2 forcing models in this paper and [25] are compared. For the alternative model, background CO_2 concentrations are taken from Table VIII of [25] for the years 2000 to 2100, with stable concentrations after 2100 of 685 ppm by volume. With a devaluation rate of 3%, results from the two models are nearly

identical. Differences of less than 0.3% are observed in relative ATR and fractional CO_2 contributions. Results differ more significantly with a devaluation rate of zero. The relative ATRs of designs B, C, and D are 4, 6, and 10% lower when calculated with varying background CO_2 concentrations. The fractional contributions of CO_2 are also lower with this alternative model. There are two observations worth noting about these results. First, the assumed scenario for background CO_2 concentrations is far more important for zero devaluation rates because all CO_2 far-future impacts are included. Second, the assumption of varying background CO_2 concentrations diminishes the impacts of future aircraft CO_2 emissions (only in the case of $r = 0$), because as background concentrations increase, each unit of CO_2 emissions causes a smaller fractional increase in atmospheric CO_2.

Alternative Aircraft Design Climate Metrics

ATR is proposed as a climate metric for the application of aircraft design. However, other metrics could be developed to serve the same purpose. Analysis is performed for two alternative metrics, each based on the same aircraft emissions scenario of H years of constant emissions followed by zero emissions.

The first is an integrated normalized RF metric, similar to GWP [14]. This metric, referred to as average RF response (ARFR), is defined as in Eqs. (1) and (16), where RF^* replaces ΔT. The weighting function given in Eq. (2) is applied. The second alternative is an endpoint metric: $\Delta T_{\mathrm{sust},H}$ is the temperature change after H years of sustained emissions and is similar to GTP [14]. Results for the relative performance of designs A, B, C, and D, as measured with these alternative metrics, are provided in Table 5.

Results for the relative climate impacts measured by the metrics ATR and ARFR are nearly identical for a given weighting function. With the LTR climate model presented in this paper, normalized RF and temperature change are distinguished from one another by a convolution operation with the function given in Eq. (15). Compared with RF, which is experienced more immediately after emissions are

Table 5 Climate performance with alternative impact-based metrics of example aircraft on a typical 1000 n mile mission

	Design A	Design B	Design C	Design D
Performance				
Relative $\mathrm{ARFR}_{30,r=0}$	1	0.90	0.81	0.72
Fraction of $\mathrm{ARFR}_{30,r=0}$ from $CO_2/NO_x/AIC$, %[a]	65/14/20	74/5/20	84/3/13	98/0/1
Relative $\mathrm{ARFR}_{30,r=3}$	1	0.76	0.55	0.31
Fraction of $\mathrm{ARFR}_{30,r=3}$ from $CO_2/NO_x/AIC$, %[a]	23/33/42	32/16/51	44/14/39	81/9/6
Relative $\Delta T_{\mathrm{sust},30}$	1	0.73	0.51	0.25
Fraction of $\Delta T_{\mathrm{sust},30}$ from $CO_2/NO_x/AIC$, %[a]	14/40/45	19/22/57	29/23/46	61/26/8

[a]Percentages do not add to 100 because of rounding and because small forcings (H_2O, soot, and sulfate) are not included.

released, temperature change is a lagged response. With nonzero devaluation rates, contributions from long-lived gases CO_2 and CH_4 are slightly higher for relative ARFR than relative ATR. This occurs because the magnitude of impacts from long-lived gases are diminished more by long-term devaluation weighting in a temperature metric than in a RF metric. However, this effect is minor and leads to differences in the contributions of CO_2, NO_x, and AIC of 2 to 7% for $r = 3\%$. With no long-term devaluation, CO_2 contributions are 1 to 3% greater for relative ARFR than for relative ATR, because CO_2 forcing does not decay to zero within the finite integration period and the lag in temperature response.

Measuring relative impacts with $\Delta T_{\text{sust},30}$ yields results that are very similar to those measured by ATR with $3\% < r < \infty$. This is expected for two reasons. First, both metrics quantify temperature change; therefore, the relative contributions of emissions at the end of the operating lifetime are equal. Second, endpoint metrics such as $\Delta T_{\text{sust},30}$ exclude impacts occurring after the operation ends, just as ATRs with moderately high devaluation rates devalue postoperation impacts.

These results demonstrate that measurements of climate performance are essentially insensitive to choice of metric between the options of integrated ΔT, integrated RF, and endpoint ΔT for the specified emissions scenario. The differences in results with each of these metrics lies primarily in the weighting of short-lived and long-lived effects, which can be adjusted within the ATR framework using weighting function parameters r and t_{max}.

Climate impacts could be quantified more simply and with less uncertainty using a metric based on direct emission quantities. Without applying a climate model, the total impacts of different aircraft emissions cannot be combined and, instead, the effects of CO_2, NO_x, and AIC must be considered separately. As previously described, because of the disparate sources of aircraft climate forcing and dependence of impacts on ambient conditions, emissions-based metrics are less useful than RF- and temperature-based metrics. Nonetheless, aircraft climate impacts could be estimated by total emitted CO_2 or NO_x, for example. If CO_2 emissions are applied as a climate metric, then designs B, C, and D would be assessed to have worse climate performance than design A, despite causing considerably smaller discounted and undiscounted temperature changes, as shown in Table 3. Similarly, basing climate impacts on mission NO_x emissions leads to the conclusion that design A has lower climate impacts than design D. Designing aircraft to limit individual emission quantities, rather than total resulting RF or temperature change, leads to configurations that cause considerably greater total RF and temperature change [32,33].

Conclusions

A metric is needed to assess the climate performance of various aircraft designs. The ATR metric quantifies the lifetime temperature change experienced due to operation of a particular aircraft. This quantity can be estimated using a climate model of any complexity, but linear climate models enable quick calculation of ATR and are appropriate for aircraft conceptual design studies. The climate model presented here accounts for the variation in NO_x and AIC impacts with cruise altitude. Alternative metrics based on the same emissions scenario and measuring integrated RF or endpoint temperature change yield similar results to ATR.

The example presented demonstrates that, for the assumptions we have adopted here, there is a significant disparity in climate performance of aircraft designed for the same mission requirements. Compared with an aircraft designed exclusively for minimum operating costs, reductions in ATR of 10–50% are achievable for aircraft with approximately 1% higher operating costs. These savings are achieved through considerable reductions in short-term impacts from ozone production and AIC with small increases to CO_2 emissions. Moreover, nearly the same ATR reduction can be achieved by flying at lower altitudes with a conventional aircraft** or

with a low-altitude aircraft design; however, the fuel burn and operating cost penalties are twice as high for the conventional aircraft. Because the impacts of NO_x emissions and contrail formation are sensitive to emission location, design cruise altitude has a powerful effect on the total climate impacts of individual aircraft. If AIC impacts were eliminated (through improved estimates of cloud effects or application of technology), then ATR reductions of 30–60% could be achieved with an operating cost penalty of 0.4% through more moderate reductions in speed and altitude (for the time weighting and other metric assumptions adopted for this example calculation).

This study also assesses the scientific uncertainty associated with ATR calculations. By determining the probability distributions of model parameters, the probability distribution for the output climate metric can also be found using paired Monte Carlo analysis. Results from the example study demonstrate that the uncertainty is not too large to make conclusions about the relative climate performance of competing designs.

Appendix

This Appendix contains information for the parameters used in the linear climate model. Best estimate values and probability distributions are provided in Tables A1–A4. These tables also cite references for the value and distribution information of each parameter.

Table A1 provides information for parameters used in computing CO_2 RF. Fifteen percent uncertainty bounds are assumed for each CO_2 parameter based on the IPCC statement that calculation of integrated RF using this CO_2 model yields a total uncertainty of 15% [5]. Thus, the uncertainty of individual parameters is overestimated.

Table A2 lists parameter information used in calculating RF caused by NO_x emissions. Following [1], NO_x-induced RF coefficients [A_{CH_4}, $A_{O_{3L}}$, and $(RF_{\text{ref}}/E_{\text{ref}})_{O_{3S}}$] are 50% correlated. All other uncertain parameters are independent. Best estimate values for A_{CH_4} and $A_{O_{3L}}$ are computed based on the method outlined in [19], using averaged results of Stevenson et al. in Table 4 of [38]. Uncertainty bounds given in [28] for f_{CH_4} and f_{O_3} are assumed to correspond to a 66% likelihood range.

Table A3 gives parameter information used in calculating RF from AIC and H_2O, SO_4, and soot emissions. Uncertainty bounds given in [28] for f_{H_2O} and f_{AIC} are assumed to correspond to a 66% likelihood range. Additionally, [5] states that there is not a consensus on the best estimate or distribution of f_{soot}. Based on studies discussed in Sec. 2.8.5.6 of [5], a best estimate of 0.7 is assumed with a 66% likelihood that the parameter is within a factor of two of this estimate.

Table A4 lists parameter information used in calculating temperature change. Probability distributions for these parameters are inferred based on the variation between four different temperature impulse response functions described in [10,37,43,44]. S is an uncertain parameter, but this uncertainty is excluded from the example study in this paper, because it has no effect on relative climate impact.

Table A1 CO_2 parameter values and distributions based on Sec. 2.10.2 of [5]

CO_2 parameter	Best estimate	Distribution: 90% likelihood range
A_{CO_2}	1.80×10^{-15} (W/m^2) /(kg CO_2)	Normal: $\{1.53 \times 10^{-15}, \quad 2.07 \times 10^{-15}\}$
α_{c1}	0.259	Normal: $\{0.220, \quad 0.298\}$
α_{c2}	0.338	Normal: $\{0.287, \quad 0.389\}$
α_{c3}	0.186	Normal: $\{0.158, \quad 0.214\}$
τ_{c1}	172.9 yr	Lognormal: $\{150, \quad 199\}$
τ_{c2}	18.51 yr	Lognormal: $\{16.1, \quad 21.3\}$
τ_{c3}	1.186 yr	Lognormal: $\{1.03, \quad 1.36\}$

**Conventional aircraft designs refer to aircraft designed to fly at typical altitudes and speeds for minimum operating costs.

Table A2 NO_x parameter values and distributions

NO_x	Best estimate	Distribution: 90% likelihood range	Best estimate source	Distribution source
A_{CH_4}	-5.16×10^{-13} (W/m²)/(kg NO_x)	Lognormal: {-8.60×10^{-14}, -3.10×10^{-12}}	Marais et al. [19]	Lee et al. [1]
$A_{O_{3L}}$	-1.21×10^{-13} (W/m²)/(kg NO_x)	Lognormal: {-3.86×10^{-14}, -3.78×10^{-13}}	Marais et al. [19]	Lee et al. [1]
f_{CH_4}	1.18	Normal: {0.977, 1.38}	Ponater et al. [27]	Grewe and Stenke [28]
f_{O_3}	1.37	Normal: {0.662, 2.08}	Ponater et al. [27]	Grewe and Stenke [28]
$(RF_{ref}/E_{ref})_{O_{3S}}$	1.01×10^{-11} (W/m²)/(kg NO_x)	Lognormal: {3.24×10^{-12}, 3.17×10^{-11}}	Sausen et al. [4]	Lee et al. [1]
τ_n	12.0 yrs	Normal: {10.2, 13.8}	IPCC [5] (Sec. 7.4.5.2.1)	IPCC [5] (Sec. 7.4.5.2.1)

Table A3 H_2O, SO_4, soot, and AIC parameter values and distributions

H_2O/SO_4/soot/AIC	Best estimate	Distribution: 90% likelihood range	Best estimate source	Distribution source
f_{H_2O}	1.14	Normal: {.550, 1.73}	Ponater et al. [27]	Grewe and Stenke [28]
f_{SO_4}	0.9	Normal: {0.412, 1.39}	IPCC [5] (Sec. 2.8.5.5)	IPCC [5] (Sec. 2.8.5.5)
f_{soot}	0.7	Lognormal: {0.212, 2.31}	IPCC [5] (Sec. 2.8.5.6)	IPCC [5] (Sec. 2.8.5.6)
f_{aic}	0.59	Normal: {.488, .692}	Ponater et al. [27]	Grewe and Stenke [28]
$(RF_{ref}/E_{ref})_{H_2O}$	7.43×10^{-15} (W/m²)/(kg H_2O)	Lognormal: {1.03×10^{-15}, 5.38×10^{-14}}	IPCC [3] (Tables 3.2 and 6.1)	Lee et al. [1]
$(RF_{ref}/E_{ref})_{SO_4}$	-1.00×10^{-10} (W/m²)/(kg SO_4)	Lognormal: {-1.65×10^{-11}, -6.10×10^{-10}}	IPCC[3] (Sec. 6.4.1 and Table 6.1)	Lee et al. [1]
$(RF_{ref}/E_{ref})_{soot}$	5.00×10^{-10} (W/m²)/(kg soot)	Lognormal: {8.23×10^{-11}, 3.04×10^{-9}}	IPCC[3] (Tables 3.2 and 6.1)	Lee et al. [1]
$(RF_{ref}/L_{ref})_{AIC}$	2.21×10^{-12} (W/m²)/n mile	Lognormal: {8.39×10^{-13}, 5.82×10^{-12}}	Stordal et al. [40]	Lee et al. [1]

Table A4   Temperature change model parameter values and distributions

Temperature model parameter	Best estimate	Distribution: 90% likelihood range	Best estimate source	Distribution source
RF_{2xCO_2}	3.70 W/m²	Normal: {3.33, 4.07}	IPCC [5] (Sec. 2.3.1)	IPCC [5] (Sec. 2.3.1)
S	3.0 K	Lognormal: {1.49, 6.03}	IPCC [5] (Box 10.2)	IPCC [5] (Box 10.2)
α_t	0.595	Lognormal: {0.397, 0.893}	Boucher and Reddy [37]	[a]
τ_{t1}	8.4 yrs	Lognormal: {4.2, 16.8}	Boucher and Reddy [37]	[a]
τ_{t2}	409.5 yrs	Lognormal: {205, 819}	Boucher and Reddy [37]	[a]

[a]Probability distributions are inferred based on the variation between four different temperature impulse response functions described in [10,37,43,44].

Acknowledgments

References

[1] Lee, D. S., Fahey, D. W., Forster, P. M., Newton, P. J., Wit, R. C., Lim, L. L., Owan, B., and Sausen, R., "Aviation and Global Climate Change in the 21st Century," *Atmospheric Environment*, Vol. 43, Nos. 22–23, 2009, pp. 3520–3537.
doi:10.1016/j.atmosenv.2009.04.024

[2] Brasseur, G., Cox, R., Hauglastaine, D., Isaksen, I., Lelieveld, J., Lister, D., Sausen, R., Schumann, U., Wahner, A., and Wiesen, P., "European Scientific Assessment of the Atmospheric Effects of Aircraft Emissions," *Atmospheric Environment*, Vol. 32, No. 13, 1998, pp. 2329–2418.
doi:10.1016/S1352-2310(97)00486-X

[3] Intergovernmental Panel on Climate Change, *Aviation and the Global Atmosphere*, Cambridge Univ. Press, Cambridge, England, U.K., 1999.

[4] Sausen, R., Isaksen, I., Grewe, V., Hauglustaine, D., Lee, D. S., Myhre, G., Kohler, M. O., Pitari, G., Schumann, U., Stordal, F., and Zerefos, C., "Aviation Radiative Forcing in 2000: An Update on IPCC (1999)," *Meteorologische Zeitschrift;Acta Scientiarium Naturalium Universitatis Normalis Hunanensis*, Vol. 14, No. 4, 2005, pp. 555–561.
doi:10.1127/0941-2948/2005/0049

[5] Intergovernmental Panel on Climate Change, *Climate Change 2007: The Physical Science Basis, Contribution of Working Group I to the Fourth Assessment Report of the Intergovernmental Panel on Climate Change*, Cambridge Univ. Press, Cambridge, England, U.K., 2007.

[6] Intergovernmental Panel on Climate Change, *Climate Change 2007 Synthesis Report*, Cambridge Univ. Press, Cambridge, England, U.K., 2007.

[7] Wuebbles, D. J., Yang, H., and Herman, R., "White Paper on Climate Metrics and Aviation: Analysis of Current Understanding and Uncertainties," Federal Aviation Admin., 2009.

[8] Wuebbles, D., Gupta, M., and Ko, M., "Evaluating the Impacts of Aviation on Climate Change," *Eos, Transactions, American Geophysical Union*, Vol. 88, No. 14, 2007, pp. 157–168.
doi:10.1029/2007EO140001

[9] Fuglestvedt, J., Bernsten, T. K., Godal, O., Sausen, R., Shine, K. P., and Skodvin, T., "Metrics of Climate Change: Assessing Radiative Forcing and Emission Indices," *Climatic Change*, Vol. 58, No. 3, 2003, pp. 267–331.
doi:10.1023/A:1023905326842

[10] Shine, K. P., Fuglestvedt, J. S., Hailemariam, K., and Stuber, N., "Alternatives to the Global Warming Potential for Comparing Climate Impacts of Emissions of Greenhouse Gases," *Climatic Change*, Vol. 68, No. 3, 2005, pp. 281–302.
doi:10.1007/s10584-005-1146-9

[11] Shine, K. P., Bernsten, T. K., Fuglestvedt, J. S., Skeie, R. B., and Stuber, N., "Comparing the Climate Effect of Emissions of Short- and Long-Lived Climate Agents," *Philosophical Transactions of The Royal Society. Series A, Mathematical, Physical, and Engineering Sciences*, Vol. 365, No. 1856, 2007, pp. 1903–1914.
doi:10.1098/rsta.2007.2050

[12] Tol, R. S., Bernsten, T. K., O'Neill, B. C., Fuglestvedt, J. S., Shine, K. P., Balkanski, Y., and Makra, L., "Metrics for Aggregating the Climate Effect of Different Emissions: A Unifying Framework," Economic and Social Research Inst. Working Paper No. 257, Dublin, 2008.

[13] Forster, P., and Rogers, H., "Metrics for Comparison of Climate Impacts from Well Mixed Greenhouse Gases and Inhomogeneous Forcing such as Those from UT/LS Ozone, Contrails and Contrail-Cirrus," Federal

Aviation Admin. Aviation Climate Change Research Initiative, Technical Rept., 2009.

[14] Fuglestvedt, J., Shine, K., Bernsten, T., Cook, J., Lee, D., Stenke, A., Skeie, R., Velders, G., and Waitz, I., "Transport Impacts on Atmosphere and Climate: Metrics," *Atmospheric Environment*, Vol. 44, No. 37, 2010, pp. 4648–4677.
doi:10.1016/j.atmosenv.2009.04.044

[15] Intergovernmental Panel on Climate Change, *Expert Meeting on the Science of Alternative Metrics*, Cambridge Univ. Press, Cambridge, England, U.K., 2009.

[16] Nordhaus, W. D., and Boyer, J., *Warming the World: Economic Models of Global Warming*, MIT Press, Cambridge, MA, 2000.

[17] Tol, R. S., "Estimates of the Damage Costs of Climate Change, Part I: Benchmark Estimates," *Environmental and Resource Economics*, Vol. 21, No. 1, 2002, pp. 47–73.
doi:10.1023/A:1014500930521

[18] Kandlikar, M., "Indices for Comparing Greenhouse Gas Emissions: Integrating Science and Economics," *Energy Economics*, Vol. 18, No. 4, 1996, pp. 265–281.
doi:10.1016/S0140-9883(96)00021-7

[19] Marais, K., Lukachko, S. P., Jun, M., Mahashabde, A., and Waitz, I. A., "Assessing the Impact of Aviation on Climate," *Meteorologische Zeitschrift*, Vol. 17, No. 2, 2008, pp. 157–172.
doi:10.1127/0941-2948/2008/0274

[20] "Social Cost of Carbon for Regulatory Impact Analysis," U.S. Government, Interagency Working Group on Social Cost of Carbon, TR USG Executive Order 12866, 2010.

[21] Nordhaus, W. D., *A Question of Balance: Weighing the Options on Global Warming Policies*, Yale Univ. Press, New Haven, CT, 2008.

[22] Nordhaus, W., "Discounting in Economics and Climate Change: An Editorial Comment," *Climatic Change*, Vol. 37, No. 2, 1997, pp. 315–328.
doi:10.1023/A:1005347001731

[23] Hammitt, J. K., Jain, A. K., Adams, J. L., and Wuebbles, D. J., "A Welfare-Based Index for Assessing Environmental Effects of Greenhouse-Gas Emissions," *Nature*, Vol. 381, 1996, pp. 301–303.
doi:10.1038/381301a0

[24] CAEP/8 NO_x Stringency Cost-Benefit Analysis Demonstration Using APMT-IMPACTS," International Civil Aviation Org. Rept. CAEP/8-IP/30, Montreal, Feb. 2010.

[25] Sausen, R., and Schumann, U., "Estimates of the Climate Response to Aircraft CO_2 and NO_x Emissions Scenarios," *Climatic Change*, Vol. 44, Nos. 1–2, 2000, pp. 27–58.
doi:10.1023/A:1005579306109

[26] Lim, L., Lee, D., Sausen, R., and Ponater, M., "Quantifying the Effects of Aviation on Radiative Forcing and Temperature with a Climate Response Model," *Proceedings of an International Conference on Transport, Atmosphere and Climate (TAC)*, Office for Official Publications of the European Communities, Luxembourg, 2006, pp. 202–207.

[27] Ponater, M., Pechtl, S., Sausen, R., Schumann, U., and Huttig, G., "Potential of the Cryoplane Technology to Reduce Aircraft Climate Impact: A State-of-the-Art Assessment," *Atmospheric Environment*, Vol. 40, No. 36, 2006, pp. 6928–6944.
doi:10.1016/j.atmosenv.2006.06.036

[28] Grewe, V., and Stenke, A., "Airclim: An Efficient Tool for Climate Evaluation of Aircraft Technology," *Atmospheric Chemistry and Physics*, Vol. 8, No. 16, 2008, pp. 4621–4639.
doi:10.5194/acp-8-4621-2008

[29] "Guidelines for Preparing Economic Analyses," U.S. Environmental Protection Agency TR 240-R-00-003, Sept. 2000.

[30] Intergovernmental Panel on Climate Change, *Climate Change 2007: Mitigation, Contribution of Working Group III to the Fourth Assessment Report of the Intergovernmental Panel on Climate Change*, Cambridge Univ. Press, Cambridge, England, U.K., 2007.

[31] Weyant, J. P., "A Critique of the Stern Review's Mitigation Cost Analyses and Integrated Assessment," *Review of Environmental Economics and Policy*, Vol. 2, No. 1, 2008, pp. 77–93.
doi:10.1093/reep/rem022

[32] Dallara, E. S., "Aircraft Design for Reduced Climate Impact," Ph.D. Thesis, Stanford Univ., Stanford, CA, Feb. 2001.

[33] Dallara, E. S., and Kroo, I., "Aircraft Design for Reduced Climate Impact," 49th AIAA Aerospace Sciences Meeting, Orlando, FL, AIAA Paper 2011-0265, 2011.

[34] Archer, D., "Fate of Fossil Fuel CO_2 in Geologic Time," *Journal of Geophysical Research*, Vol. 110, 2005, Paper C09S05.
doi:10.1029/2004JC002625

[35] Deidewig, F., Dopelheuer, A., and Lecht, M., "Methods to Assess Aircraft Engine Emissions in Flight," *Proceedings of the 20th International Council of Aeronautical Sciences Congress*, Sorrento, Italy, 1996.

[36] Norman, P., Lister, D., Lecht, M., Madden, P., Park, K., Penanhoat, O., Plaisance, C., and Renger, K., "Development of the Technical Basis for a New Emissions Parameter Covering the Whole Aircraft Operation (NEPAIR)," European Community TR G4RD-CT-2000-00182, 2003.

[37] Boucher, O., and Reddy, M., "Climate Trade-Off Between Black Carbon and Carbon Dioxide Emissions," *Energy Policy*, Vol. 36, No. 1, 2008, pp. 193–200.
doi:10.1016/j.enpol.2007.08.039

[38] Stevenson, D. S., Doherty, R. M., Sanderson, M. G., Collins, W. J., Johnson, C. E., and Derwent, R. G., "Radiative Forcing from Aircraft NO_x Emissions: Mechanisms and Seasonal Dependence," *Journal of Geophysical Research*, Vol. 109, 2004, Paper D17307.
doi:10.1029/2004JD004759

[39] Kohler, M. O., Rädel, G., Dessens, O., Shine, K. P., Rogers, H. L., Wild, O., and Pyle, J. A., "Impact of Perturbations to Nitrogen Oxide Emissions from Global Aviation," *Journal of Geophysical Research*, Vol. 113, 2008, Paper D11305.
doi:10.1029/2007JD009140

[40] Stordal, F., Myhre, G., Stordal, E., Rossow, W., Lee, D., Arlander, D., and Svendby, T., "Is There a Trend in Cirrus Cloud Cover due to Aircraft Traffic?" *Atmospheric Chemistry and Physics*, Vol. 5, No. 8, 2005, pp. 2155–2162.
doi:10.5194/acp-5-2155-2005

[41] Rädel, G., and Shine, K. P., "Radiative Forcing by Persistent Contrails and its Dependence on Cruise Altitudes," *Journal of Geophysical Research*, Vol. 113, 2008, Paper D07105.
doi:10.1029/2007JD009117

[42] Fichter, C., Marquart, S., Sausen, R., and Lee, D. S., "The Impact of Cruise Altitude on Contrails and Related Radiative Forcing," *Meteorologische Zeitschrift;Acta Scientiarium Naturalium Universitatis Normalis Hunanensis*, Vol. 14, No. 4, 2005, pp. 563–572.
doi:10.1127/0941-2948/2005/0048

[43] Hasselmann, K., Sausen, R., Maier-Reimer, E., and Voss, R., "On the Cold Start Problem in Transient Simulations with Coupled Atmosphere-Ocean Models," *Climate Dynamics*, Vol. 9, No. 2, 1993, pp. 53–61.
doi:10.1007/BF00210008

[44] Joos, F., Prentice, I. C., Sitch, S., Meyer, R., Hooss, G., Plattner, G.-K., Gerber, S., and Hassel-Mann, K., "Global Warming Feedbacks on Terrestrial Carbon Uptake Under the Intergovernmental Panel on Climate Change (IPCC) Emission Scenarios," *Global Biogeochemical Cycles*, Vol. 15, No. 4, 2001, pp. 891–907.
doi:10.1029/2000GB001375

[45] Schwartz, E., Baughcum, S. L., and Daggett, D. L., "Quantifying the Fuel Burn Penalties for an Operational Contrail Avoidance System," *SAE Aerotech Conference*, Seattle, WA, European Community, 2009.

[46] Stordal, F., Gauss, M., Myhre, G., Mancini, E., Hauglustaine, D., Kohler, M., Bernsten, T., Stordal, E., Iachetti, D., Pitari, G., and Isaksen, I., "Tradeoffs in Climate Effects Through Aircraft Routing: Forcing due to Radiatively Active Gases," *Atmospheric Chemistry and Physics Discussions*, Vol. 6, No. 5, 2006, pp. 10,733–10,771.
doi:10.5194/acpd-6-10733-2006

[47] Eldred, M. S., Adams, B. M., Gay, D. M., Swiler, L. P., Haskell, K., Bohnhoff, W. J., Eddy, J. P., Hart, W. E., and Watson, J.-P., *DAKOTA, A Multilevel Parallel Object-Oriented Framework for Design Optimization, Parameter Estimation, Uncertainty Quantification, and Sensitivity Analysis, Ver. 4.2 User's Manual*, Sandia National Labs., Livermore, CA, 2008.

[48] Saltelli, A., Tarantola, S., Campolongo, F., and Ratto, M., *Sensitivity Analysis in Practice: A Guide to Assessing Scientic Models*, Wiley, New York, 2004.

[49] Schwartz, E., and Kroo, I., "Aircraft Design: Trading Cost and Climate Impact," 47th AIAA Aerospace Sciences Meeting, Orlando, FL, AIAA Paper 2009-1261, 2009.

[50] Kroo, I., "An Interactive System for Aircraft Design and Optimization," AIAA Aerospace Design Conference, AIAA Paper 1992-1190, 1992.

[51] Mannstein, H., Spichtinger, P., and Gierens, K., "A Note on How to Avoid Contrail Cirrus," *Transportation Research Part D*, Vol. 10, No. 5, 2005, pp. 421–426.
doi:10.1016/j.trd.2005.04.012